Magneto-optical properties of the competing-anisotropy model system $Fe_{1-x}Co_xCl_2$. I. Linear birefringence and refractive index

W. Nitsche and W. Kleemann
Angewandte Physik, Universität Duisburg, D-4100 Duisburg 1, Federal Republic of Germany
(Received 2 February 1987)

The concentration-versus-temperature phase diagram of the random antiferromagnetic mixture with competing spin anisotropies $Fe_{1-x}Co_xCl_2$ is investigated via spin-correlation functions emerging from linear-birefringence and refractive-index measurements. At the upper sharp paramagnetic-to-antiferromagnetic transition at T_{C1} the initial trigonal symmetry is preserved in the Ising regime ($x < x_t \simeq 0.28$), whereas it becomes orthorhombic in the XY range ($x > x_t$). In accordance with random-exchange critical behavior, negative exponents α of the specific heat are inferred for both regimes. Fluctuating symmetry-breaking off-diagonal correlations, $\langle S_\parallel S_\perp \rangle$, appear below T_{C1}, preceding the smeared antiferromagnetic to oblique antiferromagnetic (OAF) transition at T_{C2}. For $0.35 \leq x < 1$ these correlations lower the symmetry to monoclinic, where $[120]_h$ is the easy in-plane spin direction at all temperatures, $T < T_{C1}$. In the range $0.26 \leq x < 0.35$, however, an in-plane spin rotation by $\pm 60°$ occurs at $T < T_{C2}$, inducing a triclinic OAF phase. This is shown to originate from an $\langle S_\parallel S_\perp \rangle$-controlled balance of fourth- and sixth-order magnetocrystalline and magneto-elastic in-plane anisotropy energy terms. In accordance with an expected first-order nature of this transition, marked hysteresis is observed and twinning may be encountered. This might explain the microdomain structure deduced previously from neutron scattering data without invoking random-field effects.

I. INTRODUCTION

In the last few years much interest has been focused onto mixed antiferromagnetic systems with competing spin anisotropies, notably those of the Ising-XY type. Within the Landau theory and mean-field approximation,[1] upper and lower phase transitions (PT's) at T_{C1} and T_{C2}, respectively, are predicted. They are due to paramagnetic-to-antiferromagnetic (PM-AF) and to antiferromagnetic to oblique antiferromagnetic (AF-OAF) transitions, respectively. According to the renormalization-group theoretical study of Fishman and Aharony,[2] the corresponding phase boundaries should cross smoothly in a tetracritical point.

One of the best studied real systems of this kind has become $Fe_{1-x}Co_xCl_2$ with $0 < x < 1$. The Fe spins have Ising-like symmetry with the easy direction parallel to the **c** axis of the rhombohedral lattice, whereas the Co spins are essentially XY-like within easy planes perpendicular to the **c** axis. Hence, at low concentrations x, successive PT's of the spin components parallel ($S_\parallel$) and perpendicular ($S_\perp$) to the **c** axis are observed. At $x > x_t$, where x_t characterizes the tetracritical point, the sequence of PT's is inverted. The phase diagram was thoroughly investigated by Wong and collaborators by means of ac susceptibility, χ', neutron scattering,[3] and, more recently,[4] magnetic specific heat, c_m. In zero magnetic field the upper PT's are sharp. Cusplike second-order c_m peaks at T_{C1} of Fe-rich compounds[4] remind us of the random-exchange behavior of diamagnetically diluted Ising antiferromagnets.[5]

Much emphasis was put into elucidating the nature of the lower PT's. They appear smeared in χ'-versus-T and neutron scattering measurements,[3] but they are not visible in the c_m-versus-T curves.[4] This extreme smearing was originally explained by random-field effects.[3] An alternative explanation was found within a renormalization-group-theoretical random-anisotropy model by Oku and Igarashi.[6] Both theories are based on the existence of off-diagonal exchange between axial and planar spin components, $S_\parallel$ and $S_\perp$, respectively, which is allowed by symmetry.[7] Mössbauer-effect studies by Howes, Price, and Wiltshire,[8] and recent neutron-scattering data[4] have shown that the moments seem to be tilted throughout the AF phase prior to the AF-OAF phase transition. Hence, the smearing extends over the entire temperature range $T_{C2} < T < T_{C1}$. This is now believed[4] to be atypical for a random-field transition, which usually becomes smeared only in the critical region, i.e., at $T < T_{eq}$, where $T_{eq} \gtrsim T_{C2}$.[9]

In this paper we shall present further evidence for the large extension of the smearing range based on linear-birefringence (LB) measurements. These are well known to be sensitive to spin-correlation functions, as outlined already in our preliminary report.[10] In particular it proves possible to detect directly the predicted[7] $\langle S_\parallel S_\perp \rangle$ correlations, which start to grow just below T_{C1}, in agreement with recent neutron results.[4] Hence, on the time scales of both the optical and the neutron experiments, the axial and planar, respectively, symmetry of the AF phase is broken prior to the transition into the OAF phase. This agrees with recent muon-spin-rotation (μSR) data on a related system, $Fe_{0.6}Co_{0.4}TiO_3$, where the correlation time of the fluctuating spin component was established to be 10^{-7}–10^{-5} s.[11]

The OAF phase is expected to be homogeneous in

both mean-field[1] and renormalization-group treatments,[6] whereas a random-field transition should yield a domain state.[12] Very surprisingly, there is indeed evidence for the occurrence of microdomains in the OAF state. From neutron scattering[3] in the near-tetracritical range, domain sizes of a few hundred angstroms were deduced. Their origin, if not due to random fields, has remained unclear up to now. The solution of this puzzle is in our opinion provided by the weak three-state Potts symmetry of the in-plane spin component owing to the rhombohedral lattice symmetry. This was neglected in all considerations[3,4] of the zero-field behavior of $Fe_{1-x}Co_xCl_2$ up to now. From our LB data we are able to determine the easy directions of $S_\perp$. They correspond to the three hexagonal $\langle 120\rangle_h$ directions for $0.35 \le x \le 1$. In the near-tetracritical range, $0.26 \le x < 0.35$, however, new easy spin directions occur at $T < T_{C2}$. They are deduced from rotations of the optical Fresnel ellipsoid. Simultaneously, hysteresis characterizes the LB-versus-T curves in the OAF phase. Analyzing the magnetocrystalline and magneto-elastic interactions of the rhombohedral system up to sixth-order terms in the spin correlations we can explain both the initial $\langle 120\rangle_h$ and the final rotated easy directions. The latter are due to off-diagonal correlations of the type $\langle S_xS_z\rangle$ and $\langle S_yS_z\rangle$, which create new minima of the intraplanar anisotropy energy. Necessarily, the system must decay into twin domains via a first-order monoclinic-to-triclinic PT. This yields a natural explanation for the domain structure and for the hysteresis effects observed.

Another aim of this work is to investigate the suspected[3] relationship to the random-exchange PT at the sharp upper PT in more detail. We analyze both refractive-index (RI) and, for comparison, magnetic specific-heat data[13] c_m for $0 \le x \le 0.27$. The cusp observed[4] on c_m versus T for $x > 0$ is confirmed, and analysis yields a critical exponent $\alpha \sim -0.11$. This is close to the value $\alpha = -0.09$ found for the diamagnetically diluted system $Fe_{1-x}Zn_xF_2$.[5] Similar conjectures seem to apply to Co-rich mixtures by analyzing the critical behavior of the in-plane LB. On dilution by Fe^{2+} ions α seems to decrease towards negative values in accordance with the cusplike behavior of c_m.[4,13]

II. CRYSTALLOGRAPHIC AND MAGNETIC PROPERTIES

$Fe_{1-x}Co_xCl_2$ is known[3] to be particularly suitable for studying the magnetic properties of a mixture of two antiferromagnets with competing spin anisotropies. First of all it is a system with nearly invariable crystallographic properties. Both $FeCl_2$ and $CoCl_2$ crystallize in the space group $R\bar{3}m$ (D_{3d}^5) with nearly identical lattice constants. The hexagonal lattice vectors $\hat{\mathbf{x}}_h \| [100]_h$, $\hat{\mathbf{y}}_h \| [010]_h$, and $\hat{\mathbf{z}}_h \| [001]_h$, along with one of the three possible Cartesian coordinate frames built up by $\hat{\mathbf{x}} \| [100]_h$, $\hat{\mathbf{y}} \| [120]_h$, and $\hat{\mathbf{z}} \| [001]_h$, are shown in Fig. 1. Both compounds are antiferromagnets with Néel temperatures $T_N = 24.6$ K for $CoCl_2$ and $T_N = 23.4$ K for $FeCl_2$, respectively. $FeCl_2$ behaves like a 3D Ising system (3D denotes three dimensional) with the easy axis parallel to $[001]_h$, while $CoCl_2$ corresponds to a 3D XY system with the easy plane $(001)_h$. Strictly speaking, $CoCl_2$ exhibits in-plane easy axes along the equivalent hexagonal $\langle 120\rangle_h$ directions as evidenced first by Wilkinson *et al.*[14]

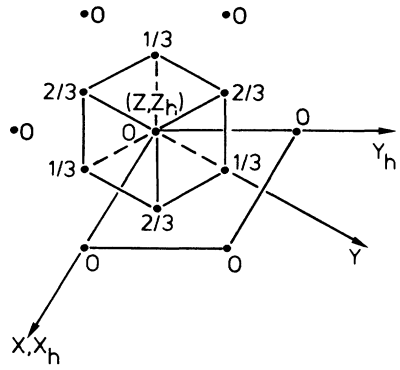

FIG. 1. Projection of the Fe^{2+} and Co^{2+} ions of $Fe_{1-x}Co_xCl_2$ within the hexagonal unit cell onto the **c** plane. The unit cell consists of three layers of Fe^{2+} and Co^{2+} ions, respectively, denoted by 0, $\frac{1}{3}$, and $\frac{2}{3}$. The axes of the hexagonal unit cell are denoted $\mathbf{x}_h$, $\mathbf{y}_h$, and $\mathbf{z}_h$. The LB calculations are done within a reference frame denoted **x**, **y**, and **z** (see Appendix A).

III. EXPERIMENTAL PROCEDURE

Single crystals of $Fe_{1-x}Co_xCl_2$ were grown by the Bridgman technique from the anhydrous compounds $FeCl_2$ and $CoCl_2$. The concentrations x were probed at different crystal sections by use of atomic absorption spectroscopy with an absolute accuracy of $\Delta x = \pm 0.005$. At intermediate x we find the concentrations of Co decreasing from the top of the crystal to the bottom tip with a typical concentration gradient of $\Delta x/\Delta l = 0.012/\text{cm}$. In order to remove residual strains the single crystals were annealed for 2 weeks at 200 °C in a HCl atmosphere. For storage the hygroscopic crystals are kept in paraffin oil to protect them against moisture. Samples were prepared by cleaving parallel to the **c** planes of the extremely soft crystals. The samples used for LB and RI measurements are thin plates with a thickness of typically 0.1–0.2 mm. The LB as well as the RI are measured using a sensitive compensation method as described by Schäfer and Kleemann.[15] The sample position is controlled by the help of a polarizing microscope, and the measurements are restricted by a diaphragm to sample areas of about $100 \times 100\ \mu\text{m}^2$ in order to avoid smearing of the PT's by macroscopic concentration gradients. Two different orientations of the samples were used in the LB measurements of $S_\perp$-ordered samples: $\Delta n(0)$ denotes the case where the crossed polarizers are parallel to $[100]_h$ and $[120]_h$, respectively, whereas $\Delta n(\pi/4)$ emerges from this orientation by rotating the sample by an angle $\beta = \pi/4$ around $[001]_h$. $[100]_h$ and $[120]_h$ are identified as the optically neutral directions of orthorhombic single domains, which are selected microscopically just below T_{C1}.

IV. EXPERIMENTAL RESULTS

A. Birefringence measurements

We have measured the LB appearing in the c plane of $Fe_{1-x}Co_xCl_2$ at various concentrations. The interconnection between the LB and one- and two-spin correlation functions is discussed in Appendix A. Furthermore, as analyzed in detail in Appendix B, the measured LB signal depends on the angle β between the polarizers and the indicatrix axes of the sample. It will, hence, be denoted $\Delta n(\beta)$ in the following. The experimental results of the LB for concentrations $0.35 \leq x \leq 1$ on one hand and for $0.26 \leq x < 0.35$ on the other hand show different behavior and will therefore be discussed separately.

1. $0.35 \leq x \leq 1$

The LB $\Delta n(\pi/4)$ versus T for samples with $x = 1.0$, 0.7, 0.38, and 0.35 is shown in Figs. 2(a)–2(d). In all cases we find $\Delta n(0)$ to be zero. This is depicted vicariously for $x = 0.38$ in Fig. 2(c) (curve 3), where small residual finite values are due to slight errors in adjusting $\beta = 0$ correctly within a few degrees. The dependence of $\Delta n(\pi/4)$ and of $\Delta n(0)$, respectively, on spin-correlation functions can be evaluated using Eqs. (A8) and (A9), together with (B3) and (B4) of the Appendixes. They give

$$\Delta n(0) = [R_{14}\langle S_z S_x \rangle + 2(R_{11} - R_{12})\langle S_x S_y \rangle]/n_0 \ , \tag{1}$$

$$\Delta n(\pi/4) = [(R_{11} - R_{12})(\langle S_y^2 \rangle - \langle S_x^2 \rangle) - 2R_{14}\langle S_y S_z \rangle]/n_0 \ . \tag{2}$$

From $\Delta n(0) = 0$ it can be inferred that the single- and two-ion contributions to both spin-correlation functions, $\langle S_z S_x \rangle$ and $\langle S_x S_y \rangle$, are vanishing. In order to understand the meanings of the off-diagonal spin correlation functions, $\langle S_z S_x \rangle$, $\langle S_x S_y \rangle$, and $\langle S_y S_z \rangle$, we have to note that Mössbauer investigations of Ito[16] on systems with competing spin anisotropies have unambiguously shown that the spin components of *both* types of magnetic ions order simultaneously at the respective phase

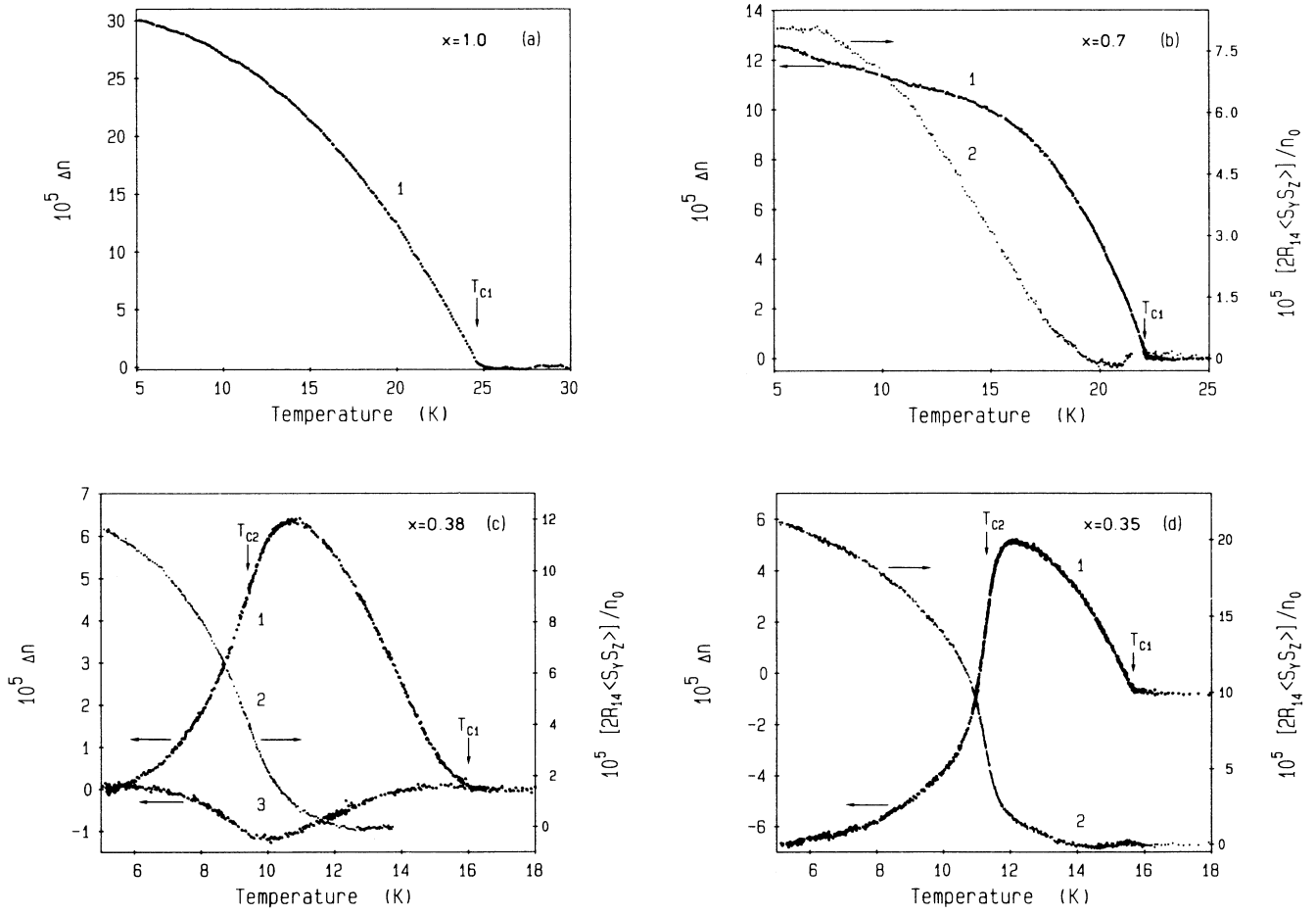

FIG. 2. Temperature dependence of $\Delta n(\pi/4)$ for (a) $x = 1.0$, (b) 0.7, (c) 0.38, and (d) 0.35 (curves labeled 1, left-hand scale). The contribution of the off-diagonal spin-correlation function $\langle S_y S_z \rangle$ to the LB is depicted by the curves labeled 2 for $x = 0.7$, 0.38, and 0.35 (right-hand scale). $\Delta n(0)$ is shown for $x = 0.38$ [(c) curve 3, left-hand scale]. The PT temperatures as determined by the onset (T_{C1}) and by the lower inflexion point (T_{C2}) of Δn, respectively, are indicated by arrows.

transitions. From that point of view S_x and S_y correspond to the respective components of both iron and cobalt ions, which order, if at all, simultaneously at the upper phase transition. The same applies to the z component, S_z, which orders at the lower phase transition. Note that according to the Fresnel ellipsoid calculations for the space group $R\bar{3}m$ of paramagnetic $Fe_{1-x}Co_xCl_2$ (see Appendix A), S_x, S_y, and S_z denote the spin components along $[100]_h$, $[120]_h$, and $[001]_h$, respectively. In this context it should be noted that the observability of LB necessitates single-domain formation, which is presumed to be due to small inherent residual strain fields. They unambiguously define the x, y, and z axes of the experiment.

From Eq. (2) spontaneous ordering along the y axis is inferred, i.e., $\langle S_y^2\rangle=\langle S_y\rangle^2+\langle\delta S_y^2\rangle$ with $\langle S_y\rangle\neq 0$, whereas $\langle S_x\rangle=0$. This is clear from $\Delta n(0)=0$, which according to Eq. (1) on the one hand implies $\langle S_xS_y\rangle=0$, but on the other hand necessarily requires $\langle S_x\rangle=0$, since $\langle S_zS_x\rangle=0$ even in the case of $\langle S_z\rangle\neq 0$ at low temperatures. The easy-spin direction, $\mathbf{S}\|[120]_h$, agrees with the neutron-scattering results of Wilkinson *et al.*[14] obtained on $CoCl_2$. It is seen that any of the LB curves of Figs. 2(b)–2(d) starts similarly as that of $CoCl_2$ [Fig. 2(a)] at its respective $T_{C1}(x)$. This indicates initial in-plane ordering, $\langle S_y^2\rangle>\langle S_x^2\rangle$, below T_{C1} as expected in Co-rich crystals,[2–4] and lowering of the symmetry from trigonal to orthorhombic. This can easily be seen from the symmetry of the ϵ tensor in the absence of off-diagonal correlations. This case is realized for pure $CoCl_2$ which lacks any off-diagonal correlations; hence

$$\Delta n(\pi/4)=[(R_{11}-R_{12})(\langle S_y^2\rangle-\langle S_x^2\rangle)]/n_0\ . \tag{3}$$

Comparing, however, the shapes of the LB curves for $x=0.35$, 0.38, and 0.7 with that obtained for $x=1$, distinct deviations are found in the low-temperature ranges (Fig. 2). They are due to the onset of off-diagonal correlations, $\langle S_yS_z\rangle$ in shorthand notation, as described by the second term of Eq. (2). Evidently these contributions grow smoothly on lowering the temperature and they are opposite in sign with respect to those described by Eq. (3). Nonvanishing $\langle S_yS_z\rangle$ signifies preferential directions of the z components of the spins and, hence, oblique spin ordering within the yz plane. Depending on the sign of $(R_{11}-R_{12})R_{14}$, the spin directions within the antiferromagnetic sublattices refer either to the first and third, or to the second and fourth, quadrants of the yz-coordinate frame, respectively. At this point it should be stressed that the LB is sensitive to both fluctuating short-range order (precursor effects[15]) and static long-range order. Its time scale is of the order 10^{-14} s, corresponding to the photon time of flight through correlated cluster volumes. Hence, it is, in principle, difficult to decide whether the lower PT appears to be smeared or sharp (see below).

In order to separate the contribution of the off-diagonal correlations $\langle S_yS_z\rangle$ to the LB $\Delta n(\pi/4)$ from that of the in-plane ordering at T_{C1}, we proceed as follows. Assuming identical critical behavior of the in-plane spin-ordering irrespective of x (small actual deviations will be discussed in Sec. V B), we have adapted the LB $\Delta n(\pi/4)$ obtained for $x=1$ to those for $x=0.35$, 0.38, and 0.7 by fitting within $0\le t\le 0.1$ using individual reduced temperature scales, $t=(T_{C1}-T)/T_{C1}$. The differences between the fitted and the actual LB's yield the $\langle S_yS_z\rangle$ terms of $\Delta n(\pi/4)$ as given by Eq. (2). These contributions to the LB are shown as curves 2 in Figs. 2(b)–2(d). Since no well-defined kinks at some sharp ordering temperatures are visible as, e.g., in the RI of NiO,[15] smeared transitions are presumed, tentatively. If we define their transition temperatures, T_{C2}, by the respective points of inflexion of the *integral* LB curves 1 (arrows in Fig. 2), lower PT's occur only for $x=0.38$ and 0.35 at $T_{C2}=8.3$ and 11.3 K, respectively. These transition temperatures agree with those obtained by Wong *et al.*[3] by means of both neutron-scattering and susceptibility measurements.

The definition of lower smeared PT's at T_{C2} seems to be justified in view of the renormalization-group calculations of Oku and Igarashi.[6] They reveal a runaway fixed point, which corresponds to the experimentally found smeared transitions. Physically the situation is characterized by nonsingular behavior of the free energy, hence implying the lack of sharp anomalies of both c_m and $d(n-n_0)/dT$ at T_{C2} as pointed out in Sec. IV B.

However, in agreement with Mössbauer measurements[8] we obtain ordering of S_z even at $x=0.7$ on the time scale of our LB experiment, whereas this is not observable on the time scale of neutron and susceptibility measurements.[3] As depicted in Fig. 2(b), the contribution of $\langle S_yS_z\rangle$ to the LB is steadily growing below T_{C1}, but a point of inflexion is lacking in Δn versus T; hence $T_{C2}<5$ K. Finally, it should be noted that $\langle S_yS_z\rangle\neq 0$ implies a lowering of the symmetry from initially orthorhombic (see above) to monoclinic. This is evident from the ϵ tensor [Eq. (A3)] and applies to the entire concentration range considered, either on the time average ($T_{C2}<T<T_{C1}$) or statically ($T<T_{C2}$).

2. $0.20\le x<0.35$

In Fig. 3 the LB-versus-T curves $\Delta n(\pi/4)$ (curves 1) as well as $\Delta n(0)$ (curves 2) are presented for concentrations $x=0.305$ and 0.29 [Figs. 3(a) and 3(b)] above the tetracritical point, and for $x=0.275$, 0.26, and 0.2 [Figs. 3(c)–3(e)] below the tetracritical point. It is seen that $\Delta n(0)$ no longer vanishes for $0.26\le x<0.35$, indicating that $\langle S_zS_x\rangle$ and/or $\langle S_xS_y\rangle$, respectively, are nonzero in this concentration range [see Eq. (1)]. Because of $\Delta n(0)\neq 0$, Eq. (2) reads, in its complete form as obtained from Eqs. (A8) and (B3)

$$\Delta n(\pi/4)=[(R_{11}-R_{12})(\langle S_y^2\rangle-\langle S_x^2\rangle)-2R_{14}\langle S_yS_z\rangle -\Delta n(0)\tan(2\alpha)/2]/[n_0\cos(2\alpha)]\ , \tag{4}$$

with α being the angle of the principal axes with respect to $[120]_h$ and $[100]_h$, respectively, as described in Eq. (A9). A common feature appearing in Figs. 3(a)–3(d) is the occurrence of hysteresis in both $\Delta n(\pi/4)$ and $\Delta n(0)$ at temperatures which we define as the PT temperatures

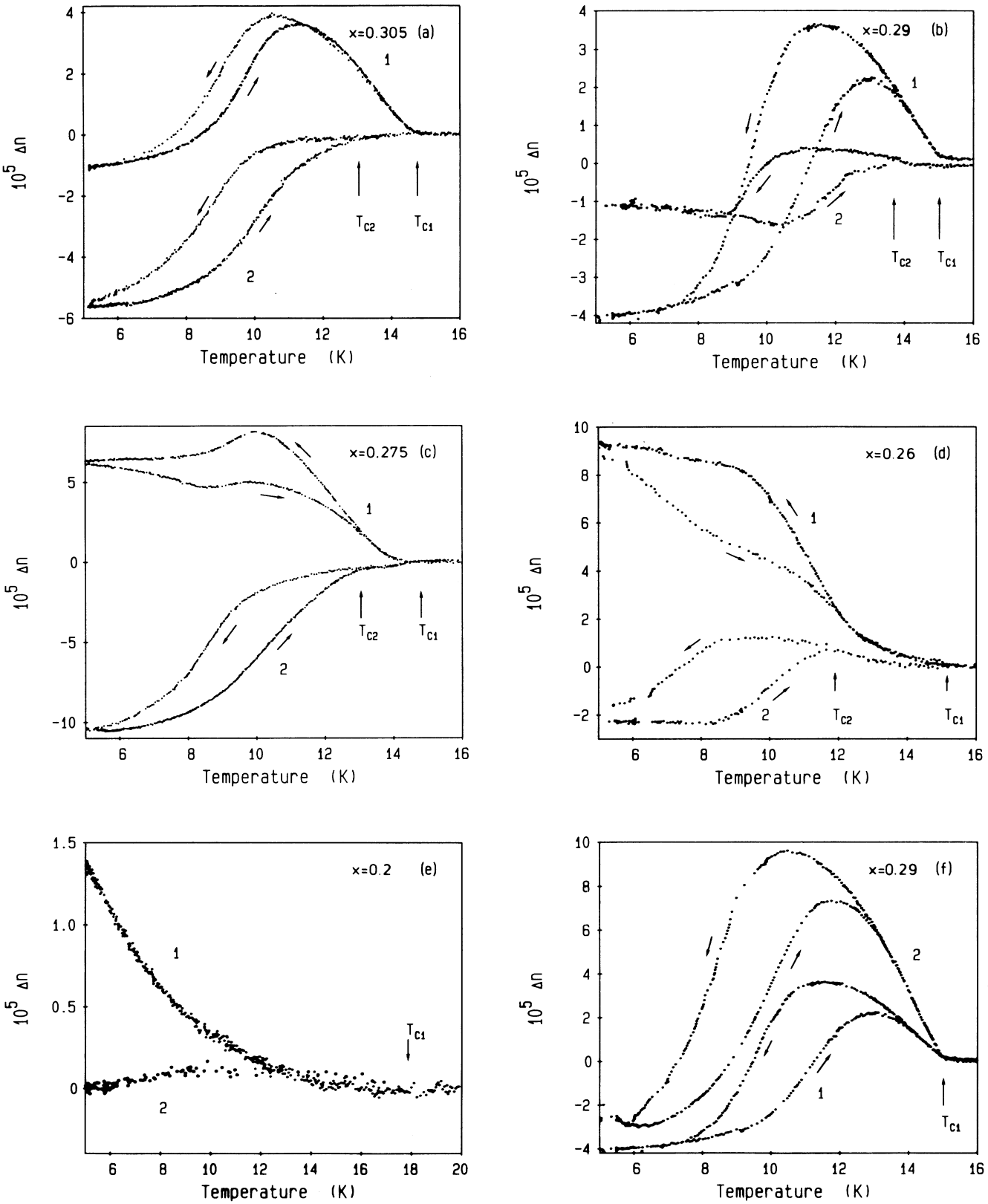

FIG. 3. Temperature dependence of $\Delta n(\pi/4)$ (curves labeled 1) and $\Delta n(0)$ (curves labeled 2) for (a) $x=0.305$, (b) 0.29, (c) 0.275, (d) 0.26, and (e) 0.2. T_{C1} and T_{C2} are indicated by arrows. Hysteresis for $T<T_{C2}$ occurs on cooling down (←) and heating up (→) the samples. For (f) $x=0.29$, $\Delta n(\pi/4)$ is depicted for an in-plane field $H=0$ (1) and $H=1.8$ kOe (2).

T_{C2} of the lower smeared PT. Thus defined, the T_{C2} values—$T_{C2}=13.2$, 13.8, 13.4, and 11.9 K for $x=0.305$, 0.29, 0.275, and 0.26, respectively—again agree well with those obtained by Wong *et al.*[3] In Fig. 3(e) hysteresis is absent, thus indicating that no lower PT occurs for $x=0.2$ above 5 K, as expected from the phase diagram.[3] The LB $\Delta n(\pi/4)$ in Figs. 3(a) and 3(b) starts to grow below T_{C1}, while $\Delta n(0)$ still vanishes for $T_{C2}<T\leq T_{C1}$. In that temperature range $\Delta n(\pi/4)$ for $x=0.305$ and 0.29 is solely due to the first term of Eq. (4). Similarly, as in the case $x\geq 0.35$ (Fig. 2), we conclude that $\langle S_y\rangle\neq 0$, whereas $\langle S_x\rangle=0$. We note that again all observations are done on strain-field-selected single domains, which necessarily have orthorhombic symmetry like the respective ϵ tensor [Eq. (A3)] in that temperature range. At this point it should be remarked that the selection of a single domain can be supported by a magnetic field applied in the c plane.[14] In Fig. 3(f) we present $\Delta n(\pi/4)$ for the sample with $x=0.29$ for $H=1.8$ kOe (curve 2) and $H=0$ [curve 1, same as curve 1 of Fig. 3(b)]. This shows that the absolute values of zero-field LB curves [Figs. 2(a)–2(d) and 3(a)–3(e)] may be masked by residual multidomain effects. On the other hand, field-selected domains exhibit more reliable LB-versus-T curves, notably in the vicinity of T_{C1}. This is essential for critical-point analysis (see Sec. V B).

The onset of $\Delta n(0)\neq 0$ at $T<T_{C2}$ implies $\langle S_zS_x\rangle\neq 0$ and/or $\langle S_xS_y\rangle\neq 0$. Since both $\langle S_y\rangle$ and $\langle S_z\rangle$ are nonvanishing owing to $\langle S_yS_z\rangle\neq 0$ from $\Delta n(\pi/4)$ [Eq. (2)], this necessarily implies also $\langle S_x\rangle\neq 0$. This, in turn, implies triclinic symmetry for $T<T_{C2}$ as can be seen from Eq. (A3) of Appendix A. According to Eqs. (4) and (1), now all off-diagonal correlation functions—$\langle S_xS_y\rangle$, $\langle S_yS_z\rangle$, and $\langle S_zS_x\rangle$—contribute to $\Delta n(\pi/4)$. This makes a quantitative evaluation particularly difficult, if not impossible.

For concentrations $x<x_t\simeq 0.28$ a smooth increase of $\Delta n(\pi/4)$ is observable between T_{C1} and the onset of hysteresis denoted as T_{C2} [Figs. 3(c) and 3(d)]. We remark that at T_{C1} spontaneous ordering of S_z is expected, whereas no long-range order of S_x,S_y should occur; hence $\langle S_x\rangle=\langle S_y\rangle=0$. Presumably in that temperature range only the first term of Eq. (4) contributes to $\Delta n(\pi/4)$, indicating strain-induced anisotropic fluctuations, $\langle S_y^2\rangle\neq\langle S_x^2\rangle$, and creating monoclinic symmetry [cf. Eq. (A3)]. In Fig. 3(e) neither $\Delta n(0)$ nor $\Delta n(\pi/4)$ for $x=0.2$ show any hysteresis effect. Within the accessible temperature range this may hint at the absence of a lower smeared PT in accordance with Wong *et al.*[3]

Finally we have to remark that both the deviation of the in-plane spin direction from $[120]_h$ and the onset of hysteresis seem to occur simultaneously at $T<T_{C2}$. As will be pointed out in detail in the discussion, we explain both features by magnetoelastic effects, which accompany the spin ordering and give rise to an orthorhombic-to-triclinic lattice transformation.

B. Refractive-index measurements and specific heat

In order to inspect the critical behavior at the upper phase transition PM-AF for concentrations $x<x_t$, we have measured the in-plane refractive index for three concentrations $x=0$, 0.2, and 0.27.[10]

From Eqs. (A6) and (A3) in Appendix A we obtain, for the average refractive index within the c plane,

$$n=\frac{n_1+n_2}{2}$$

$$=n_0+\frac{1}{2n_0}[R_{13}\langle S_z^2\rangle+\tfrac{1}{2}(R_{11}+R_{12})(\langle S_x^2\rangle+\langle S_y^2\rangle)]\ . \tag{5}$$

At the upper PT only $\langle S_z^2\rangle$ is expected to become critical, and should therefore contribute preponderantly to the critical part of the magnetic energy. Hence the critical behavior of $d(n-n_0)/dT$ should be proportional to that of the magnetic specific heat. First of all this is confirmed for pure $FeCl_2$ ($x=0$) as shown in Fig. 4, where our data are compared with c_m data of Lanusse *et al.*[17] Evidently, the short-range correlations, abbreviated as $\langle S_x^2\rangle$ and $\langle S_y^2\rangle$, which certainly enter the expressions of $d(n-n_0)/dT$ and c_m with different weights, do not disturb the proportionality over a wide temperature range. This seems to indicate their minor importance for $x=0$.

The magnetic specific heat of the solid solutions was measured by Ikeda[13] with an ac-calorimetric method on samples originating from the same single crystals as used in our LB and RI measurements. The c_m data displayed in Figs. 5 and 6 were obtained from the total specific heat[13] after subtraction of the lattice part fitted at high temperatures to that of $CdCl_2$.[17] The errors resulting from that procedure are estimated to be less than 10%. On the other hand, no correction is applied to the $d(n-n_0)/dT$ data presented in Figs. 5 and 6, assuming a flat diamagnetic background at low temperatures. It is noted that both methods yield roughly the same temperature dependences [Figs. 5(a) and 6(a)]. Slight differences in the peak temperatures, T_{C1}, may be traced back to the concentration gradients within the single

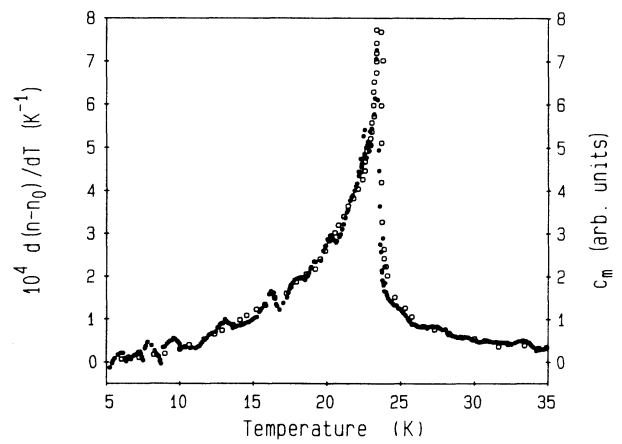

FIG. 4. Temperature dependence of $d(n-n_0)dT$ (●) and c_m (○) (Ref. 17), respectively, for $FeCl_2$ ($x=0$).

crystals supplying different samples to both experiments. Systematic noise arises in the $[d(n-n_0)/dT]$-versus-T curves owing to the optical interference method, which is sensitive to minor displacements of the sample with respect to the split light beam.[15] Nevertheless, their similarity with the c_m-versus-T curves, notably in the peak regions, is evident. We also notice good agreement with recent c_m data of Wong,[4] albeit obtained on crystals with slightly different concentrations. Plots of both $d(n-n_0)/dT$ [Figs. 5(b) and 6(b)] and c_m [Figs. 5(c) and 6(c)] versus $\log_{10}|t|$, where $t=T/T_{C1}-1$ is the reduced temperature, exhibit negative curvatures for $|t| \lesssim 10^{-2}$ ($x=0.2$), and $|t| \lesssim 10^{-1}$ ($x=0.27$), respectively. This seems to indicate cusplike behavior of the

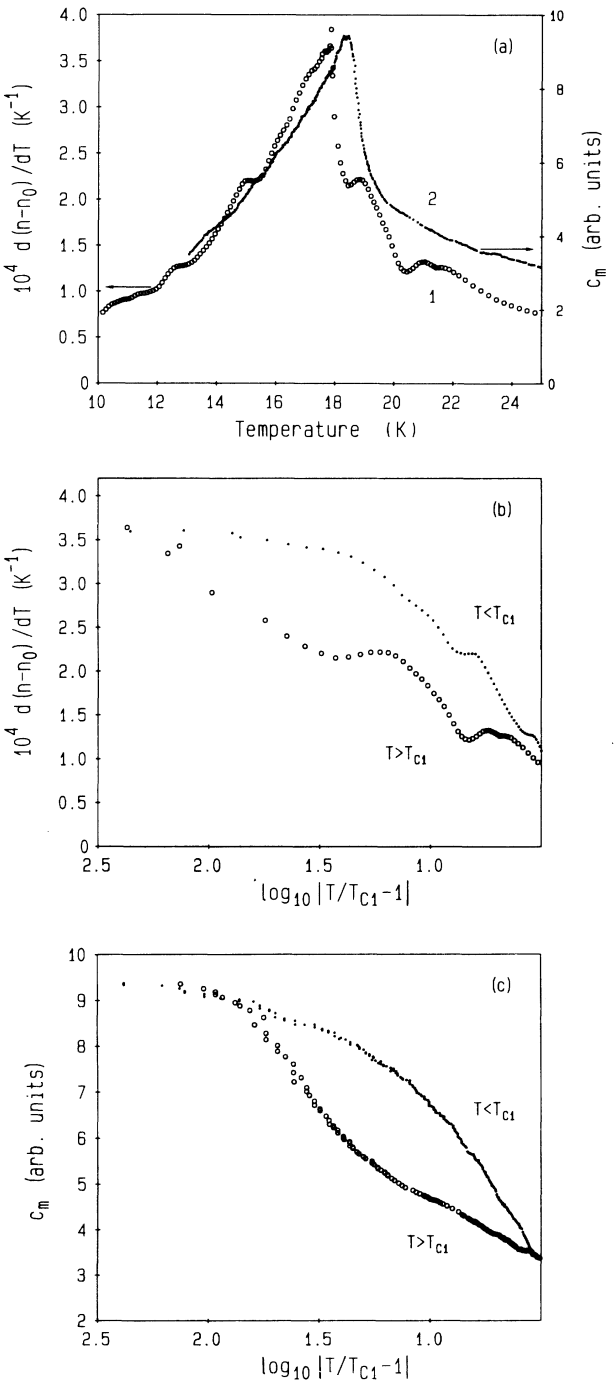

FIG. 5. (a) $d(n-n_0)/dT$ (1) and c_m (2) vs T, (b) $d(n-n_0)/dT$ vs $\log_{10}|T/T_{C1}-1|$ with $T_{C1}=17.78$ K, and (c) c_m vs $\log_{10}|T/T_{C1}-1|$ with $T_{C1}=18.33$ K for $Fe_{0.8}Co_{0.2}Cl_2$.

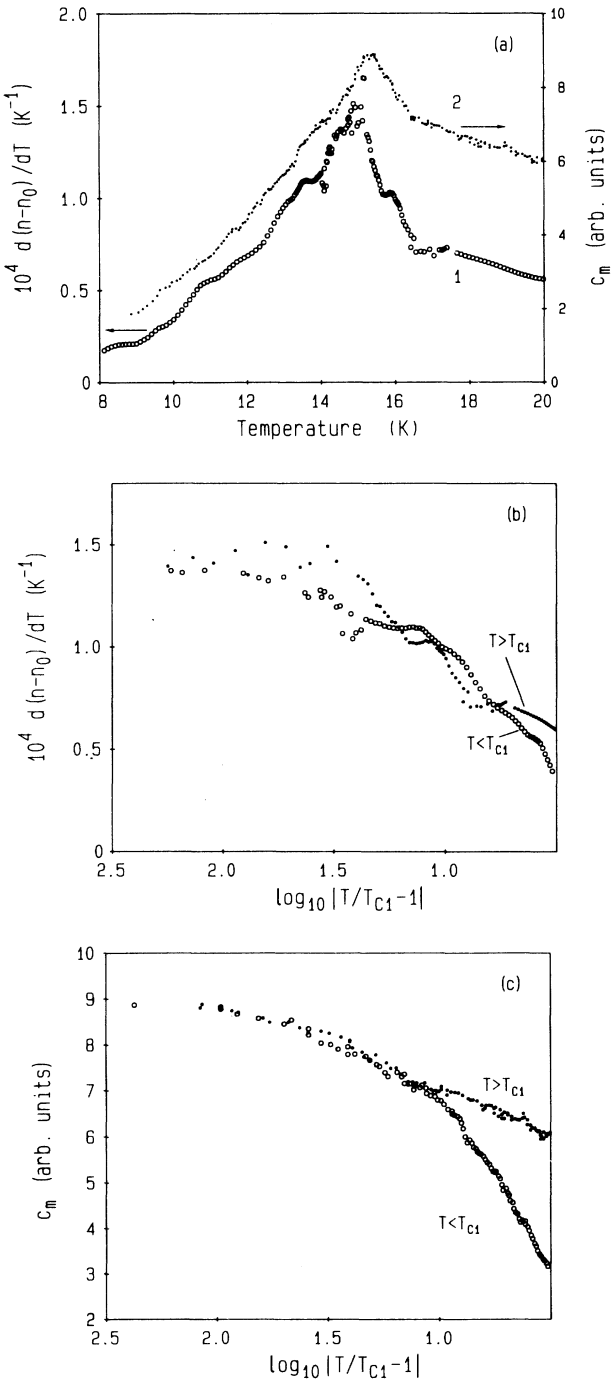

FIG. 6. (a) $d(n-n_0)/dT$ (1) and c_m (2) vs T, (b) $d(n-n_0)/dT$ vs $\log_{10}|T/T_{C1}-1|$ with $T_{C1}=14.8$ K, and (c) c_m vs $\log_{10}|T/T_{C1}-1|$ with $T_{C1}=15.32$ K for $Fe_{0.73}Co_{0.27}Cl_2$.

specific heat, i.e., critical exponents $\alpha < 0$. These are expected in the 3D random-exchange Ising-model limit.[5]

Significant differences between the "optical" and the caloric specific heat data are only remarked for $x = 0.27$, where the c_m curve exhibits an enhancement of its high-temperature tail with respect to that of $d(n-n_0)/dT$ [Fig. 6(a)]. This might hint at Co^{2+}-induced strong contributions of noncritical correlations $\langle S_x^2 \rangle$ and $\langle S_y^2 \rangle$ to the specific heat. They destroy the simple proportionality of c_m and $d(n-n_0)/dT$ for $x \lesssim x_t$. It should be noted that neither c_m nor $d(n-n_0)/dT$ indicate any clear-cut contribution due to the AF-OAF phase transition, which is expected at $T_{C2} \sim 13.3$ K for $x = 0.27$. This confirms that this transition appears to be smeared[3,4,6] without showing critical behavior.

V. DISCUSSION

A. Intraplanar anisotropy and domain formation

As outlined in Sec. IV A the birefringence measurements on $Fe_{1-x}Co_xCl_2$ are compatible with in-plane spin directions along $\langle 120 \rangle_h$ for concentration $0.35 \leq x \leq 1$. For concentrations $0.26 \leq x < 0.35$ the in-plane spin directions deviate from $\langle 120 \rangle_h$ as has been pointed out in the preceding section as well as in our previous paper.[10] In order to explain these results we have to consider the origin of the anisotropy for both compounds, $FeCl_2$ and $CoCl_2$. We remember that $FeCl_2$ is a good example for a 3D Ising antiferromagnet with the easy axis being the trigonal c axis. On the other hand, $CoCl_2$ is a good example for a 3D xy antiferromagnet with easy axes along the hexagonal $\langle 120 \rangle_h$ directions, as was first observed by Wilkinson *et al.*[14] A crystal-field approach to describe the anisotropy of both $FeCl_2$ and $CoCl_2$ was chosen by Lines.[18] On projecting an isotropic exchange Hamiltonian onto the ground states of Fe^{2+} and Co^{2+}, respectively, in a trigonal crystal field, and including spin-orbit coupling, Lines obtained the following Hamiltonian,

$$\mathcal{H}_m = -2 \sum_{\langle i,j \rangle} J^{ij} \mathbf{S}(i) \cdot \mathbf{S}(j) + D^{ij}[S_\parallel(i) S_\parallel(j) - S_\perp(i) S_\perp(j)/2] \ . \tag{6}$$

The nearest-neighbor exchange constants J and the anisotropy constants D according to Wong *et al.*[3] are $J = 4.24$ K and $D = 1.29$ K for $FeCl_2$, and $J = 12.11$ K and $D = -6.44$ K for $CoCl_2$, respectively. However, no explanation for the in-plane easy directions $\langle 120 \rangle_h$ in the case of $CoCl_2$ is given by Eq. (6).

In the following it will be shown that this requires higher-order terms than those included in Eq. (6) within a phenomenological theory of magnetocrystalline anisotropy and magneto-elastic coupling. Following the procedure given by Callen and Callen,[19] the free energy F of the system can be written as

$$F = F_m + \mathcal{H}_e + \langle \mathcal{H}_{me} \rangle + \langle \mathcal{H}_a \rangle \ . \tag{7}$$

In this relation F_m, $\mathcal{H}_e$, $\langle \mathcal{H}_{me} \rangle$, and $\langle \mathcal{H}_a \rangle$ denote the magnetic free energy obtained from Eq. (6), the elastic energy, the ensemble average of the magneto-elastic energy, and that of the fourth- and sixth-order magnetocrystalline energy, respectively. The elastic and magneto-elastic contributions are given by the general formula[20]

$$\mathcal{H}_e + \langle \mathcal{H}_{me} \rangle = \sum_{K,l,l',\Gamma} (\tfrac{1}{2} c_{ll'}^{\Gamma} e_K^{\Gamma,l} e_K^{\Gamma,l'} - B_{ll'}^{\Gamma} e_K^{\Gamma,l} S_K^{\Gamma,l'}) \ , \tag{8}$$

where $c_{ll'}^{\Gamma}$, $e_K^{\Gamma,l}$, $B_{ll'}^{\Gamma}$, and $S_K^{\Gamma,l'}$ are the symmetry-adapted elastic constants, strains, magneto-elastic coupling constants, and spin-correlation functions, respectively. The sums are taken over the n-dimensional ($K = 1, \ldots, n$) irreducible representations Γ, where l and l' refer to the corresponding set of basis functions. After a lengthy, but straightforward calculation following the procedure of Ref. 20 one obtains the following expression for the space group $R\bar{3}m$:

$$\mathcal{H}_e + \langle \mathcal{H}_{me} \rangle = -\frac{1}{c_{11}-c_{12}} \{ \tfrac{1}{4}[B_1(\langle S_1 \rangle - \langle S_2 \rangle) + 2B_3 \langle S_4 \rangle]^2 + (B_1 \langle S_6 \rangle + B_3 \langle S_5 \rangle)^2 \} - \frac{2}{c_{44}} \left[\tfrac{1}{4}[B_2(\langle S_1 \rangle - \langle S_2 \rangle) + B_4 \langle S_4 \rangle]^2 + \left[B_2 \langle S_6 \rangle + \frac{B_4}{2} \langle S_5 \rangle \right]^2 \right] , \tag{9}$$

where we have introduced the elastic constants c_{ij} in conventional Voigt notation and abbreviated the corresponding $B_{ll'}$ by B_i. Furthermore, we have used the shorthand notations $S_1 = S_x^2$, $S_2 = S_y^2$, $S_3 = S_z^2$, $S_4 = S_y S_z$, $S_5 = S_z S_x$, and $S_6 = S_x S_y$. In the above expression the strains were eliminated under the constraint of vanishing stress. Moreover, we have neglected the elastic constants c_{13} and c_{14} for the following reason. $FeCl_2$ and $CoCl_2$, respectively, consist of covalently bonded layers which are weakly coupled prevalently by van der Waals forces along the c axis. Therefore, coupling between interplanar strain and shear, e_{zz} and e_{yz}, respectively, and in-plane stress, σ_{xx} and σ_{yy}, is expected to be negligible. Unfortunately, to our knowledge only the elastic constants c_{33}, c_{44}, and $c_{11}-c_{12}$ of $FeCl_2$ have been determined,[21] but not c_{13} and c_{14} of either $FeCl_2$ or $CoCl_2$. Treating the spins as classical vectors with $S_x = S \sin\theta \cos\phi$, $S_y = S \sin\theta \sin\phi$, and $S_z = S \cos\theta$ in a spherical reference frame, and omitting the angular brackets denoting thermal averages of the spin functions from now on, Eq. (9) may be written as

$$\mathcal{H}_e+\langle\mathcal{H}_{me}\rangle=-\frac{S^4}{c_{11}-c_{12}}(\tfrac{1}{4}B_1^2\sin^4\theta+\tfrac{1}{4}B_3^2\sin^2 2\theta+B_1B_3\sin^3\theta\cos\theta\sin 3\phi)$$
$$-\frac{S^4}{c_{44}}(\tfrac{1}{2}B_2^2\sin^4\theta+\tfrac{1}{8}B_4^2\sin^2 2\theta+B_2B_4\sin^3\theta\cos\theta\sin 3\phi)\ . \tag{10}$$

By use of the results of Fieschi and Fumi[22] the fourth- and sixth-order terms of the magnetocrystalline energy of trigonal systems can be evaluated similarly as in the case of hexagonal systems[23] as

$$\langle\mathcal{H}_a\rangle=K_0+K_1\sin^2\theta+K_2\sin^4\theta+K_3\sin^6\theta+K_4\cos\theta\sin^3\theta\sin 3\phi+K_5\sin^6\theta\cos 6\phi+O^6(\cos\theta,\cos^3\theta)\ , \tag{11}$$

with six anisotropy constants K_0, K_1, K_2, K_3, K_4, and K_5. The last term of Eq. (11) denotes sixth-order contributions containing factors $\cos\theta$ and $\cos^3\theta$, respectively. These are assumed to be negligible in comparison with the fourth-order K_4 term. In order to determine the in-plane spin directions only the fourth-order term with the anisotropy constant K_4 and the sixth-order term with K_5 are important. Note that the first of these two terms vanishes for $\theta=90°$, i.e., in the case that $\langle S_z\rangle=0$.

We obtain the in-plane spin directions by minimizing both the magnetocrystalline and the magneto-elastic energy with respect to ϕ, according to

$$\frac{d}{d\phi}(\langle\mathcal{H}_{me}\rangle+\mathcal{H}_e+\langle\mathcal{H}_a\rangle)=0\ . \tag{12}$$

Inserting Eqs. (10) and (11) into Eq. (12) we obtain

$$3\left[K_4-\frac{S^4B_1B_3}{c_{11}-c_{12}}-\frac{S^4B_2B_4}{c_{44}}\right]\sin^3\theta\cos\theta\cos 3\phi$$
$$-6K_5\sin^6\theta\sin 6\phi=0\ . \tag{13}$$

In the limit $\langle S_z\rangle=0$, equivalent to $\theta=90°$, Eq. (13) reduces to

$$6K_5\sin 6\phi=0\ . \tag{14a}$$

Depending on the sign of the anisotropy constant K_5, we obtain the easy directions in the c-plane

$$\phi=\begin{cases}30°,90°,150°,\ldots, & \text{for } K_5>0\ , \quad (14b)\\ 0°,60°,120°,\ldots, & \text{for } K_5<0\ . \quad (14c)\end{cases}$$

Hence, in the case $\langle S_z\rangle=0$, only the sixth-order term of the magnetocrystalline energy gives rise to in-plane spin anisotropy. Experimentally we obtain, for $x>x_t$ and at $T<T_{C1}$, the in-plane spin direction $[120]_h$, indicating $\phi=90°$. Therefore the anisotropy constant K_5 must be positive in order to describe the experimental results. It is easily verified that the in-plane anisotropy energy, E_{intra}, yields a minimum at $\theta=\phi=90°$. Using the ϕ-dependent part of $\mathrm{H}_e+\langle\mathrm{H}_{me}\rangle+\langle\mathrm{H}_a\rangle$ according to Eqs. (10) and (11),

$$E_{\text{intra}}=\left[K_4-\frac{S^4B_1B_3}{c_{11}-c_{12}}-S^4\frac{B_2B_4}{c_{44}}\right]$$
$$\times\sin^3\theta\cos\theta\sin 3\phi+K_5\sin^6\theta\cos 6\phi\ , \tag{15}$$

one obtains $E_{\text{intra}}(\theta=\phi=90°)=-K_5$. Note that only three different in-plane directions, described by pairs of azimuthal angles, $\phi=90°$ and 270°, 30° and 210°, or 150° and 330°, respectively, can be distinguished in an antiferromagnet owing to the staggering of its magnetization. One of these may be selected by virtue of favorably directed internal strains, as detected, e.g., by well-defined LB. It defines what henceforth will be denoted as $[120]_h$ or y direction, which enters, e.g., the crystal optical calculation in Appendix A.

The OAF phase is characterized by $\langle S_z\rangle\neq0$ or $\theta\neq90°$, respectively. Hence, both terms in Eq. (15) have to be inspected in order to determine the minimum of E_{intra}. It is seen that only the angles ϕ given by Eq. (14a) satisfy the condition (13), irrespective of the values of θ and of the coefficients involved. Experimentally, we find $\phi=90°$ for $0.35\leq x\leq0.7$ at all temperatures below T_{C1} (Sec. IV A; Fig. 2). Hence, the energy minimum remains determined by the negative last term in Eq. (15), as in the case $\theta=90°$. Consequently the first term must be either negative, as well, or positive, but smaller than $|K_5\sin^6\theta\cos 6\phi|$. A decision on this question is brought about by the experimental observation that ϕ deviates from 90° for $0.26\leq x<0.35$ and at $T<T_{C2}$ (Sec. IV A; Fig. 3). This seems to indicate that the minimum at $\phi=90°$ disappears by virtue of a growing positive contribution due to the first term in Eq. (15). At the same time the adjacent minima, at $\phi=30°$ and 150°, respectively, become more pronounced and provoke spin reorientation (see below) giving rise to $\Delta n(0)\neq0$ (Fig. 3).

These conjectures are based on the assumption that the coefficients of the angular functions in Eq. (15) are essentially independent of x. This applies to K_5 and to the factor in large parentheses, which also comes out to be positive, since $90°<\theta\leq180°$.[8] Hence, the driving force giving rise to the spectacular rotation of the anisotropy axes must be connected with the increasing z ordering of the spins on increasing the concentration of Fe^{2+} ions. This effect is indeed dramatic in the near-tetracritical range, $0.26\leq x<0.35$, as evidenced by the θ values obtained from Mössbauer measurements at low temperatures.[8] On the contrary, only weak variations with x are found for $\theta\gtrsim90°$ in the range $0.35\leq x<1$.[8] Roughly speaking, it is the factor $\cos\theta$ of the first term in Eq. (15), which determines the minimum of E_{intra} to change from $\phi=90°$ to 30°, 150°, or even 270° at a certain threshold value $\theta=\theta_0$. From the Mössbauer data[8] of the angular direction of the molecular exchange field of $Fe_{1-x}Co_xCl_2$, we estimate an approximate value, $\theta_0\sim130°$, which is obtained at $x<0.35$.

The mechanism of the spin reorientation into new

equilibrium positions, $\phi \neq 90°$, is connected with hysteresis as shown in Figs. 3(a)–3(d). For example, in the case of $x = 0.305$ [Fig. 3(a)] the sample must be cooled to below a temperature $T_1 \sim 0.85 T_{C2}$ in order to observe nonvanishing $\Delta n(0)$. This might be connected with metastability of the $\phi = 90°$ state with respect to the absolute minima of E_{intra} occurring at $\phi = 30°$ and 150°. As usual in first-order phase transitions, there exists a lower transition temperature, T_1, where the metastability of the high-temperature phase gets lost and the transition *must* occur. For symmetry reasons the occurrence of domains of either orientation, $\phi = 30°$ and 150°, are expected. $\phi = 270°$ domains are less probable owing to enhanced energy barriers arising at $\phi = 210°$ and $-30°$, respectively. If the domains are distributed in equal proportions, $\Delta n(0)$ should virtually vanish. This situation may be encountered in the vicinity of T_1. At low temperatures, however, one of the new spin directions seems to dominate by virtue of residual strain fields with favorable directions. Then we find considerable, albeit sample-dependent $\Delta n(0)$, signals, and an appreciable decrease of $\Delta n(\pi/4)$ (Fig. 3). On heating, on the other hand, the new domain distribution remains stable up to an upper metastability limit, T_{C2}. At this temperature, where $\langle S_z \rangle$ is virtually vanishing and the minima at both $\phi = 30°$ (or 150°) *and* 90° become equivalent again [see Eq. (15)], the initial selection mechanism of the orthorhombic domains becomes active and favors the original $\phi = 90°$ domain. In this context the reproducibility of LB measurements on once selected sample sections should be kept in mind.

The above-described mechanism is suggested to apply to the OAF phase occurring at both $x > x_t$ and $x < x_t$. In the latter case in-plane ordering is absent at temperatures $T_{C2} < T < T_{C1}$. However, strain-induced anisotropic fluctuations are observed [Figs. 3(c) and 3(d)], which unambiguously define the initial $\phi = 90°$ direction. The transition into the $\phi \neq 90°$ domains should then proceed as in the case $x > x_t$. It should be stressed that this transition necessarily leads to a mixture of equivalent domains, unless one type of them is selected by symmetry-breaking strains. Such a multidomain mixture was found by Wong *et al.*[3] from neutron scattering on an $x = 0.295$ system. Domain sizes of a few hundred angstroms were estimated. Moreover, they also found hysteresis, albeit less clear than in our LB data (Fig. 3), in the range $0.29 \leq x \leq 0.35$. In agreement with our present interpretation, Wong *et al.*[3] qualitatively proposed magneto-elastic interactions to be the origin of these effects.

However, they also invoked the random-field mechanism first proposed by Mukamel.[7] By virtue of off-diagonal exchange coupling [cf. Eq. (A1)] those spin components ordering at the PM-AF transition are expected to generate local random fields, which act on the spin component that orders at the AF-OAF transition. By cooling under these random fields this PT becomes smeared and should result in a domain state.[12] Alternatively, however, the smearing of the lower PT's in both $Fe_{1-x}Co_xCl_2$ and $Fe_{1-x}Co_xBr_2$ was explained within a random anisotropy model by Oku and Igarashi.[6] They concluded that random fields very probably do not play a prominent role at the lower PT's. Our present investigations have, moreover, shown that even the development of a domain state does not require the existence of random fields. By using macroscopic symmetry arguments we find that a domain state necessarily emerges in virtue of magneto-elastic and magnetocrystalline interaction involving off-diagonal spin-spin correlations. It must, hence, be concluded that contrary to former expectations[3] the competing anisotropy system $Fe_{1-x}Co_xCl_2$ is not a good candidate to investigate random-field effects. Analyzing new c_m and neutron-scattering data Wong[4] recently drew the same conclusion. In agreement with our interpretation of the LB results and with recent μSR data,[11] the broad smearing of the lower PT's over the entire range $T_{C2} < T < T_{C1}$, on time scales shorter than about 10^{-6} s, was taken as untypical for random-field transitions. Minor effects due to random fields, however, cannot be excluded either.

B. Random-exchange behavior

As discussed above, the upper PT's are characterized by the ordering of one spin components, which simultaneously establishes fluctuating perpendicular correlations. It is, hence, interesting to investigate possible consequences on the critical behavior. In the range $x < x_t$ reliable data of both $d(n - n_0)/dT$ [Fig. 6(b)] and c_m [Fig. 6(c)] are available for $x = 0.27$. From the c_m data we obtain $\alpha = -0.11 \pm 0.01$ within the reduced temperature range $0.03 < |t| < 0.003$, where $T_{C1} = 15.32$ K. This is similar to the results obtained for the diluted antiferromagnet $Fe_{0.6}Zn_{0.4}F_2$ with $\alpha = -0.09 \pm 0.005$.[5] The close resemblance of the critical exponents α suggests that $Fe_{0.73}Co_{0.27}Cl_2$ may be considered a random-exchange system at T_{C1}, as also conjectured by Wong[4] from the cusplike shapes of his c_m data. Off-diagonal correlations, $\langle S_\parallel S_\perp \rangle$, hence, do not seem to change the critical exponent α expected for the random-exchange 3D dimensional Ising model. However, they seem to modify the amplitude ratio, whose value $A/A' \sim 1$ [Fig. 6(c)] differs appreciably from that expected, $A/A' \sim 0.6$.[5] The situation is similar for $x = 0.2$ [Fig. 5(c)], where cusplike behavior of c_m, however, is only observable for $t < 10^{-2}$, very probably preceded by pure-to-random crossover at larger $|t|$.[5] Owing to the scarcity and the poor quality of the data in the cusp range, the value of a α could not reliably be extracted. This is unfortunate, since very probably in this case, lacking any transition into the OAF phase at low temperatures, the resemblance with a random-exchange system should even be more certain than the near-tetracritical case $x = 0.27$.

For concentrations above the tetracritical point, $x > x_t$, we have attempted to investigate the critical behavior at the upper PT by use of in-plane LB data. These proved to be at least 1 order of magnitude more accurate than RI data taken on the same sample, as expected.[15] Within a single domain the critical behavior at $T < T_{C1}$ is given by[24]

$$\Delta n \propto |t|^{\tilde{\beta}}, \tag{16}$$

with $\tilde{\beta}=2-\alpha-\psi$, which α and ψ are the specific-heat and the crossover exponents, respectively.

First of all we have determined the critical behavior of the pure system, $CoCl_2$. Both natural, i.e., strain-selected [Fig. 2(a)], and magnetic-field-induced (see Sec. IV A) orthorhombic single domains yield identical values, $\tilde{\beta}=0.81\pm0.02$, on fitting their LB data within the range $0.1<|t|<0.004$ to the relation (16). Evidently a small intraplanar magnetic field (here: $0\leq H\leq 0.18$ T) does not affect the critical behavior of this system, similarly as experienced on the cubic antiferromagnet $KNiF_3$.[25] As outlined in Sec. IV A the main purpose of applying a finite field is to conveniently produce excellent single domains.

Disregarding its small three-state Potts anisotropy, $CoCl_2$ is believed to belong to the 3D XY universability class. By use of the corresponding exponents $\alpha=-0.0079\pm0.003$[26] and $\psi=1.175$ (crossover from 3D XY to 3D Ising)[27] one calculates $\tilde{\beta}=0.833\pm0.003$. Inserting an experimental value, $\psi=1.17\pm0.02$, obtained by Rohrer and Gerber,[28] one finds $\tilde{\beta}=0.82\pm0.02$. Both values agree satisfactorily with our experimental result, thus confirming the prevalent XY symmetry of the spins of $CoCl_2$.

In the mixed systems, $x_t<x<1$, perfect single domains are much less probable in naturally strained samples than in the pure system. As shown for $x=0.29$ in Fig. 3(f), the rounding of the LB near T_{C1} (curve 1) is essentially removed on application of an in-plane field, $H=0.18$ T (curve 2). On closer inspecting the critical data, however, the analysis according to relation (16) is still hampered by residual rounding in the range $|t|<0.02$. Moreover, the onset of off-diagonal correlations just below T_{C1} systematically deforms the curvature of the LB curve compared to that which would be solely due to the intraplanar spin ordering (see Sec. IV A). This must be kept in mind when discussing our result on the $x=0.29$ sample. We obtain $0.87<\tilde{\beta}<0.90$ from LB data within $0.1\leq|t|\leq0.02$, slightly varying with the field direction, $0\leq\phi\leq90°$.

Despite the scatter of the data an increase of $\tilde{\beta}$ with respect to that of pure $CoCl_2$ is quite obvious. This seems to indicate a decrease of α toward more negative values in accordance with Harris's criterion[29] and with the observations on diluted 3D Ising systems.[5] Unfortunately a quantitative analysis is not possible at present, since, to the best of our knowledge, neither α, nor ψ have been predicted theoretically for the random-exchange 3D xy model.

VI. CONCLUSION

The phase diagram[3] of the random-anisotropy system $Fe_{1-x}Co_xCl_2$ has been confirmed by measurements of the optical birefringence and of the refractive index. In agreement with specific-heat data,[4] evidence is found of the random-exchange nature of the sharp upper phase transition at T_{C1}. Negative critical exponents, α, seem to emerge for both Ising-type $S_\parallel$ ordering at $x<x_t$ ($x_t=0.28$) and XY-type $S_\perp$ ordering at $x>x_t$.

Fluctuating correlations of $S_\perp$ ($S_\parallel$) occurring for $x<x_t$ ($x>x_t$) just below T_{C1} indicate an unusually large precursor range, $T_{C2}<T<T_{C1}$, prior to the AF-OAF transition at T_{C2}. This is a consequence of symmetry-allowed off-diagonal spin-spin coupling,[7] which manifests itself by easily distinguishable contributions to the LB. Evidence was also derived from neutron-scattering,[3,4] Mössbauer,[8] and (on a related system) μSR (Ref. 11) data.

The smeared nature[6] of the PT at T_{C2}, expected for $0.25<x<0.40$,[3] is confirmed by the smooth variation with T of the respective spin component and, for $x<0.27$, by the absence of any anomaly at T_{C2} in $d(n-n_0)/dT$ versus T. Fe^{2+}-rich mixtures, $0.26\leq x\leq0.305$, moreover, exhibit hysteresis, and a rotation of the intraplanar spin direction at $T\leq T_{C2}$. This is due to enhanced $S_\parallel$ correlations giving rise to first-order transitions into triclinic twin domains on cooling, and thus contrasts with the continuous orthorhombic-to-monoclinic transformation found for $0.35\leq x<1$. Calculations of the intraplanar anisotropy involving magnetocrystalline and magneto-elastic interactions up to sixth order reveal that the intraplanar spin directions may indeed be controlled by $\langle S_\parallel S_\perp\rangle$. At a certain threshold value spontaneous rotations by $\pm60°$ do arise. On one hand this behavior proves the relevance of higher-order spin correlations to the model system $Fe_{1-x}Co_xCl_2$ (only second-order contributions were considered up to now[3,4,8]). On the other hand, a natural explanation is found for the occurrence of a microdomain structure in the OAF phase without invoking random-field effects.[3,7]

Random-field effects arise more clearly, if an external field is applied along the c axis, as has recently been demonstrated by Wong.[4] Very interesting phenomena concerning the H-T phase diagram, critical behavior at $T_{C1}(H)$, and field-induced metastability have been explored for $Fe_{1-x}Co_xCl_2$ by ourselves using the Faraday rotation technique,[30] and will be published separately.[31]

ACKNOWLEDGMENTS

Many thanks are due to Professor H. Ikeda, Tokyo, for measuring the specific heat on some of our samples for sake of comparison with our refractive-index data. Moreover, we are greatly indebted to H. M. Kuss, who measured the concentrations of the mixed crystals, and to H. Junge and F. J. Schäfer for valuable technical assistance.

APPENDIX A: SPIN CORRELATIONS AND CRYSTAL OPTICS

Since the works of LeGall *et al.*[32] and Smolenskii *et al.*[33] it is well known that the optical refractive indices and the corresponding linear optical birefringence are sensitive to spin-correlation functions. According to Borovik-Romanov *et al.*,[34] one may consider the dependence of the electrical energy of the radiation per unit volume on the spin correlations according to

$$\omega_e = \tfrac{1}{2} \sum_{i,j=x,y,z} \left[\epsilon_{ii} E_i E_i + \tfrac{1}{2} \sum_{l,l',\gamma,\delta=x,y,z} (R_{ij\gamma\delta} < S_l^{\gamma} S_{l'}^{\delta} > E_i E_j) \right] . \tag{A1}$$

In this relation ϵ_{ij} represents the optical permittivity tensor components, E_i the electric field of the radiation, $R_{ij\gamma\delta}$ the magneto-optic tensor components, and $\langle S_l S_{l'} \rangle$ the spin-correlation functions, respectively. Single-ion ($l = l'$) as well as two-ion ($l \neq l'$) contributions are included. In the following we shall omit the indices l, l' for sake of brevity. In the particular case of the space group $R\bar{3}m$ ($= D_{3D}^5$) seven independent magneto-optic tensor components exist.[34] Using the shorthand notations $xx = 1$, $yy = 2$, $zz = 3$, $yz = 4$, $xz = 5$, and $xy = 6$, we obtain via

$$\epsilon_{ii} = \frac{\partial \omega_e}{\partial E_i \partial E_i} \quad \text{and} \quad \epsilon_{ij} = \frac{1}{2} \frac{\partial \omega_e}{\partial E_i \partial E_j} \tag{A2}$$

the following relation between the permittivity tensor components and the spin-correlation functions:

$$\begin{pmatrix} \epsilon_1 - \epsilon_o \\ \epsilon_2 - \epsilon_o \\ \epsilon_3 - \epsilon_e \\ \epsilon_4 \\ \epsilon_5 \\ \epsilon_6 \end{pmatrix} = \begin{pmatrix} R_{11} & R_{12} & R_{13} & R_{14} & 0 & 0 \\ R_{12} & R_{11} & R_{13} & -R_{14} & 0 & 0 \\ R_{31} & R_{31} & R_{33} & 0 & 0 & 0 \\ R_{41} & -R_{41} & 0 & R_{44} & 0 & 0 \\ 0 & 0 & 0 & 0 & R_{44} & 4R_{41} \\ 0 & 0 & 0 & 0 & R_{14}/2 & R_{11} - R_{12} \end{pmatrix} \begin{pmatrix} \langle S_x^2 \rangle \\ \langle S_y^2 \rangle \\ \langle S_z^2 \rangle \\ \langle S_y S_z \rangle \\ \langle S_z S_x \rangle \\ \langle S_x S_y \rangle \end{pmatrix} . \tag{A3}$$

We have chosen a coordinate system with $\hat{\mathbf{x}} \| [100]_h$, $\hat{\mathbf{y}} \| [120]_h$, and $\hat{\mathbf{z}} \| [001]_h$, and $\epsilon_o = n_o^2$ and $\epsilon_e = n_e^2$ are related to the ordinary and extraordinary refractive indices of the paramagnetic phase, n_o and n_e, respectively. The propagation of light in a crystal is described by the Fresnel ellipsoid given by

$$\mathbf{x} \underline{\epsilon} \mathbf{x} = 1 , \tag{A4}$$

where we have denoted the permittivity tensor by $\underline{\epsilon}$ and the space vector by $\mathbf{x} = (x, y, z)$. Accommodated to the experimental situation, where only the in-plane refractive indices and birefringence, respectively, can be measured owing to the layered structure of our samples, we confine our calculation to the x-y plane approximately described by

$$(x \quad y) \begin{pmatrix} \epsilon_{xx} & \epsilon_{xy} \\ \epsilon_{xy} & \epsilon_{yy} \end{pmatrix} \begin{pmatrix} x \\ y \end{pmatrix} = 1 . \tag{A5}$$

From this relation we obtain the principal axes, $\epsilon'_{1,2}$, of the Fresnel ellipsoid given by

$$\epsilon'_{1,2} = \frac{\epsilon_{xx} + \epsilon_{yy}}{2} \mp [\epsilon_{xy}^2 + \tfrac{1}{4}(\epsilon_{xx} - \epsilon_{yy})^2]^{1/2} . \tag{A6}$$

They are rotated by the angle α with respect to the crystallographic x and y axes, respectively, according to

$$\tan(2\alpha) = \frac{2\epsilon_{xy}}{\epsilon_{xx} - \epsilon_{yy}} . \tag{A7}$$

We are now able to express the in-plane birefringence with respect to the principal axes by spin-correlation functions on inserting (A3) into (A6) and (A7), and obtain

$$\begin{aligned} \Delta n_{12} &= \frac{1}{n_0}(\epsilon'_1 - \epsilon'_2) \\ &= \frac{1}{n_0}[(R_{11} - R_{12})(\langle S_y^2 \rangle - \langle S_x^2 \rangle) \\ &\quad - 2R_{14}\langle S_y S_z \rangle]/\cos(2\alpha) . \end{aligned} \tag{A8}$$

The angle α is given by

$$\tan(2\alpha) = -\frac{R_{14}\langle S_z S_x \rangle + 2(R_{11} - R_{12})\langle S_x S_y \rangle}{(R_{11} - R_{12})(\langle S_y^2 \rangle - \langle S_x^2 \rangle) - 2R_{14}\langle S_y S_z \rangle} . \tag{A9}$$

APPENDIX B: BIREFRINGENCE MEASUREMENTS

The birefringence was measured using a sensitive compensation method as described by Schäfer and Kleemann.[15] In Fig. 7 the arrangement of the optical components and the orientation of their principal axes within planes perpendicular to the light propagation are shown.

In the usual case, $\beta = \pi/4$, the compensation condition is $\varphi_c = -\varphi_s$, where φ_c and φ_s are the phase retardations of the compensator and of the sample, respectively. It is obtained by nulling the intensity component I_ω at the modulator frequency, ω, using lock-in technique.[15] In

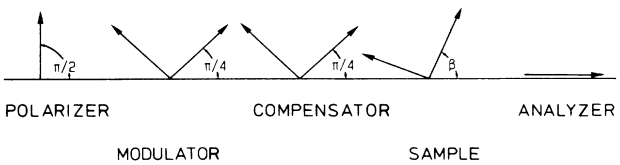

FIG. 7. Scheme of the setup for measuring the LB (see text).

the general case, $\beta \neq \pi/4$, this condition no longer denotes $\varphi_0 = -\varphi_s$. Using the Jones-matrix formalism[35] a straightforward calculation yields

$$I_\omega = \tfrac{1}{2} I_0 J_1(\varphi_m)\sin(\omega t)\left[\cos(4\beta)\sin^2\left[\frac{\varphi_s}{2}\right] + \cos^2\left[\frac{\varphi_s}{2}\right]\sin\varphi_c + \sin\varphi_s \sin(2\beta)\cos\varphi_c\right] . \quad \text{(B1)}$$

In this formula φ_m is the phase amplitude of the photoelastic modulator operating at $\omega = 2\pi \times 50$ kHz. $J_1(\varphi_m)$ is the first Bessel function. The compensation condition $I_\omega = 0$ now reads

$$\varphi_c = \arctan\left[-\frac{\sin\varphi_s \sin(2\beta)}{\cos^2(\varphi_s/2) + \cos(4\beta)\sin^2(\varphi_s/2)}\right] , \quad \text{(B2)}$$

which yields $\varphi_c = -\varphi_s$ in the limit $\beta = \pi/4$.

Within the context of our present investigation (see Secs. III and IV) we are interested in the following two cases.

(a) If the principal axes of the sample are only slightly turned with respect to those of the compensator, i.e., $\beta \sim \pi/4$ and $\alpha \ll \pi/4$, we obtain

$$\varphi_c \simeq -[1 - \tan^2(2\alpha)/2]\varphi_s . \quad \text{(B3)}$$

Keeping in mind the relation $\varphi_s = 2\pi l \Delta n_{12}/\lambda$, where l and λ are the sample thickness and the light wavelength, respectively, Eq. (B3) describes the quantity denoted as $\Delta n(\pi/4)$ in Secs. II and III. It may be evaluated by inserting the relations (A8) and (A9).

(b) If the principal axes are slightly turned with respect to those of the polarizer and analyzer, respectively, i.e. $\beta \sim 0$ and $\alpha \ll \pi/4$, we obtain

$$\varphi_c \simeq -[\tan(2\alpha)]\varphi_s . \quad \text{(B4)}$$

This case refers to the quantity defined as $\Delta n(0)$ and may be evaluated as described above.

[1] F. Matsubara and S. Inawashiro, J. Phys. Soc. Jpn. **42**, 1529 (1977); **46**, 1740 (1979); Y. Someya, *ibid.* **50**, 3897 (1981).
[2] S. Fishman and A. Aharony, Phys. Rev. B **18**, 3507 (1978).
[3] P. Z. Wong, P. M. Horn, R. J. Birgeneau, and G. Shirane, Phys. Rev. B **27**, 428 (1983).
[4] P. Z. Wong, Phys. Rev. B **34**, 1864 (1986).
[5] R. J. Birgeneau, R. A. Cowley, G. Shirane, H. Yoshizawa, D. P. Belanger, A. R. King, and V. Jaccarino, Phys. Rev. B **27**, 6747 (1983).
[6] M. Oku and H. Iagarashi, Prog. Theor. Phys. **70**, 1493 (1983).
[7] D. Mukamel, Phys. Rev. Lett. **46**, 845 (1981).
[8] B. D. Howes, D. C. Price, and M. C. K. Wiltshire, J. Phys. C **17**, 3669 (1984).
[9] A. Aharony, J. Magn. Magn. Mater. **54-57**, 27 (1986).
[10] W. Nitsche and W. Kleemann, J. Magn. Magn. Mater. **54-57**, 37 (1986).
[11] E. Torikai, A. Ito, Y. Takeda, K. Nagamine, K. Nishiyama, Y. Syono, and H. Takei, Solid State Commun. **58**, 839 (1986).
[12] J. G. Grinstein and S.-k. Ma, Phys. Rev. B **28**, 2588 (1983); J. Villain, Phys. Rev. Lett. **52**, 1543 (1984); R. Bruinsma and G. Aeppli, *ibid.* 1547 (1984).
[13] H. Ikeda (unpublished).
[14] M. K. Wilkinson, J. W. Cable, E. O. Wollan, and W. C. Köhler, Phys. Rev. **113**, 497 (1959).
[15] F. J. Schäfer and W. Kleemann, J. Appl. Phys. **57**, 2606 (1985).
[16] A. Ito, Hyperfine Interact. **27**, 81 (1986).
[17] M. C. Lanusse, P. Carrara, A. R. Fert, G. Mischler, and J. P. Redoulès, J. Phys. (Paris) **33**, 429 (1972).
[18] M. E. Lines, Phys. Rev. **131**, 540 (1963).
[19] E. Callen and H. B. Callen, Phys. Rev. **139**, A455 (1965).
[20] M. E. Lines, Phys. Rep. **55**, 133 (1979).
[21] G. Gorodetsky, A. Shaulov, and V. Volterra, Phys. Rev. B **13**, 1205 (1976).
[22] R. Fieschi and F. G. Fumi, Nuovo Cimento **10**, 865 (1953).
[23] W. P. Mason, Phys. Rev. **96**, 302 (1954).
[24] J. Ferré and G. A. Gehring, Rep. Progr. Phys. **47**, 513 (1984).
[25] P. Nordblad, D. P. Belanger, A. R. King, V. Jaccarino, and H. J. Guggenheim, J. Magn. Magn. Mater. **31-34**, 1093 (1983).
[26] L. C. Le Guillou and J. Zinn-Justin, Phys. Rev. Lett. **39**, 95 (1977).
[27] M. E. Fisher, in *Magnetism and Magnetic Materials—1974 (San Francisco)*, Proceedings of the 20th Annual Conference on Magnetism and Magnetic Materials, AIP Conf. Proc. **24**, edited by C. D. Graham, G. H. Lander, and J. J. Rhyne (AIP, New York, 1975), p. 273.
[28] H. Rohrer and Ch. Gerber, Phys. Rev. Lett. **28**, 909 (1977).
[29] A. B. Harris, J. Phys. C **7**, 1671 (1974).
[30] W. Kleemann, A. R. King, and V. Jaccarino, Phys. Rev. B **34**, 479 (1986).
[31] W. Nitsche and W. Kleemann (unpublished).